A new method for estimating evaporative losses from hot springs using chloride and deuterium as tracers.

A Thesis

Presented in Partial Fulfilment of the Requirements for the

Degree of Master of Science

with a

Major in Geological Sciences

in the

College of Graduate Studies

University of Idaho

by

Megan M. Aunan

Major Professor: Jerry P. Fairley, Ph.D.

Committee Members: Thomas Williams, Ph.D.; Erika Rader, Ph.D.

Department Administrator: Leslie Baker, Ph.D

August 2019

Authorization to Submit Thesis

This thesis of Megan Marie Aunan, submitted for the degree of Master of Science with a major in Geology and titled "A new method for estimating evaporative losses from hot springs using chloride and deuterium as tracers," has been reviewed in final form. Permission, as indicated by the signatures and dates given below, is now granted to submit final copies to the College of Graduate Studies for approval.

Major Professor

_____Date_____
Jerry P. Fairley, Ph.D.

Committee Members

_____Date_____
Thomas J. Williams, Ph.D.

_____Date_____
Erika Rader, Ph.D.

Department Administrator

_____Date_____
Leslie Baker, Ph.D.

Abstract

Estimates of the total heat budget of a thermal area is typically derived using the basic principles of mass and energy balance but the parameters neccessary to make such estimates are expensive and difficult to measure. Commonly, investigators use chemical tracers as proxies for parameters allowing the mass transfer by advective transport (flowing water) to be estimated. In spite of the available methodology for predicting advective fluxes, the heat transferred by vapor during evaporation has not yet been calculated. Evaporative processes are generally elevated in thermal areas due to large temperature gradients between surface water and the atmosphere, as well as convective transport at the spring surface by wind. The effect of evaporation on mass transfer is likely negligible but its effect on energy transfer is likely much greater and, therefore, requires further investigation. Expanding on published tracer techniques, I introduce a new method to quantify evaporation losses by intiating an instantaneous increase of two chemical tracers in two hot springs in The Borax Lake Thermal Area, one tracer is a conservative species that does not leave the liquid water to partition with vapor during evaporation (chloride) and the other is non-conservative and will partition with vapor to leave the liquid water (deuterium). By contrasting each tracers return to normal background levels, the model can predict the rates at which water is entering the spring in the subsurface, liquid water is leaving the spring, and water vapor is lost by evaporation. In addition, the model calculates the volume involved with subsurface mixing and estimates the concentration of chloride and the δD-values of the incoming liquid and the vapor leaving the springs. An extension of the model calculates an energy balance and indicates that the effect of evaporation on energy transfer due to the latent heat of evaportation can account for 16-20 % of the advective heat transported by the liquid water. This method provides an easy, inexpensive technique to quantify the energy loss by evaporation in a thermal area.

Acknowledgements

I would first like to thank my advisor, Dr. Jerry P. Fairley, for his support during my time at University of Idaho, both as an undergraduate and a graduate student. Dr. Fairley was always available to help me whether it was for my research, classwork, or in planning the numerous field seasons that we worked together. Throughout writing this thesis, Dr. Fairley encouraged me to write this paper as my own but provided the perfect amount of guidance when I encountered any roadblocks.

I would also like to thank my committee members, Dr. Thomas Williams and Dr. Erika Rader for their helpful comments on my research and writing. To Dr. Peter Larson from Washington State University for his wealth of knowledge in stable isotopes and thermal areas. To Cary Lindsey, Ella Titterington, and TJ Sorenson for their help with field sampling, and to the Renfrew Fellowship of the University of Idaho College of Science and the National Science Foundation Fellowship for their funds used to purchase the deuterium for the experiment.

Finally, I must express my forever gratitude to my husband for his unfailing support and encouragement throughout my years in college and patience thoughout the very long process. My accomplishments would not have been possible without him.

Table of Contents

Authorization to Submit Thesis ..... **ii**

Abstract ..... **iii**

Acknowledgements ..... **iv**

Table of Contents ..... **v**

List of Tables ..... **vi**

List of Figures ..... **vii**

1 Introduction **1**

1.1 Introduction 1

1.2 Site Information 4

2 Methods **5**

2.1 Model Development 5

2.1.1 Chloride mass balance model 7

2.1.2 Chloride model parameterization 9

2.1.3 Deuterium mass balance model 12

2.1.4 Deuterium model parameterization 15

2.2 Chemistry 16

3 Results **18**

3.1 Results 18

4 Discussion **24**

4.1 Discussion 24

4.2 Uncertainties 28

5 Conclusion 29

5.1 Conclusion 29

References 29

List of Tables

3.1 Relative humidity and air temperature. 19

3.2 Spring temperatures measured at the beginning and end of each experiment. . . 19

3.3 Elapsed time with corresponding chloride concentrations and δD. * indicates points removed from the model. 20

3.4 Parameter values used in the models. (1) from [18] (2) from [12] 21

3.5 Parameters calculated from the calibrated model. 21

List of Figures

1.1 Map of the Alvord Basin with Borax Lake, spring locations north of the lake. Taken from [8] 4

2.1 Chloride concentration for B1180 as a function of time (.) and (*) marks when C is $\frac{1}{e}$ above background. 10

2.2 Chloride concentration for B1210 as a function of time (.) and (*) marks when C is $\frac{1}{e}$ above background. 10

2.3 δD values for spring B1180 as a function of time. 11

2.4 δD values for spring B1210 as a function of time. 11

3.1 Spring B1180: Measured non-dimensional chloride concentration (blue dots) and δ D (black dots) as a function of dimensionless time (τ) compared to the model values (solid black for chloride and solid purple for deuterium. 22

3.2 Spring B1210: Measured non-dimensional chloride concentration (blue dots) and δ D (black dots) as a function of dimensionless time (τ) compared to the model values (solid black for chloride and solid purple for deuterium. 23

4.1 Spring B1180 26

4.2 Spring B1210 26

CHAPTER 1

Introduction

1.1 Introduction

Energy and mass balance of thermal areas is an important tool for characterizing subsurface flowpaths, the interplay of thermal features located near to each other, and calculating the total thermal budget of a system [[11], [23], and [19]]. Most investigations of this type focus on processes in which energy and mass are moved by advective transport (flowing water). It is challenging to obtain measurements to support these studies because the required data are expensive and troublesome to collect and, therefore, necessitates the use of many assumptions such as reservoir characteristics, initial concentration and temperatures of parent fluids, or the source and fate of ground and surface waters. These difficulties lead to errors in the estimations of the total heat flux in a hydrothermal system.

As a way to circumvent these limitations, techniques are available that use conservative chemical ions as proxies for the parameters neccessary to refine calculations and have done so with success. To be considered conservative, the ion must not react by adsoprtion or exchange with host rocks, precipitate under changing conditions such as pH, temperature or evaporation, it must stay dissolved in water and not partition into the gas phase, and have an assumed or known source for any initial concentrations present. The following techniques are desirable because they are inexpensive, relatively straight forward, and have minimal ecological impact.

[6] improved estimates of heat transfer by advection in New Zealand by measuring the change in chloride concentration above and below a point where thermal waters are visibly entering a stream to refine calculations of the surface discharge of thermal waters at this location. [2] expands on this method in New Zealand at a thermal area which there is little, or no, visible discharge but an obvious high heat input. The author spiked the springs with a known amount of NaCl and recorded the change in chloride concentration over time as it

returned to background. This data was modelled to fit to an exponential decay curve and the author shows how to calculate the total mixing volume and discharge rates. This study, and many that follow, suggests a complex underground plumbing system is located beneath thermal areas. Using iodide as a tracer, [23] spiked a large hot spring in the Daisy Geyser Group and measured any changes in concentration over time in other thermal features within this group. Their research supports previously suggested reciprocal behavior between springs and geysers in the near field but also suggests that subsurface communication may occur between groups of features far away as well.

More recent, in Yellowstone National Park, [19] spiked several hot springs with deuterium and show that when combining their estimates for heat transferred by advection with previously published conductive heat flux estimates that the total heat budget for the Yellowstone caldera has been crudely underestimated. This study stands apart from previously mentioned studies because deuterium is not conservative and fractionates with water molecules as it partitions into vapor during evaporation. Although the authors used a tracer that partitions into the vapor phase during evaporation, there was no such method to include it in the thermal estimates at the time of their study.

Although these studies offer insight into the transport of heat and mass by advection, the authors neglect the transport of heat by evaporation noting there are likely errors in their estimates as a result. Due to the large amount of energy involved in phase change, it seems feasible that neglecting the latent heat by evaporation will result in errors when calculating the total thermal budget. Athough evaporation does not have much impact on calculating mass changes in a spring, it is important when in determining the amount of heat leaving a spring with the water vapor and will be demonstrated in the following sections.

Stable isotopes, δD and δ^{16}O, are powerful tools to study the evaporation of water and are used in a variety of settings such as ephemeral lakes, terminal lakes, well-mixed systems, and other large water bodies. Isotopic ratios of δD/δO in lakes show significant shifts from the meteoric water line due to the mass fractionation of isotopes during evaporation [3]. [12],

presents several case studies describing isotopic fluxes by evaporation which investigates the controls on and amount of mass fractionation but does not include the energy of the phase change of water.

The methods for calculating flux mentioned here use a single tracer in water for mass balance (Cl^-, δD, etc.) as a proxy to obtain a more complete energy balance model. By doing so, the authors improve estimates of advective heat transport but disregard the effect of evaporation on mass and energy transport. [3] and [12] suggest that combining isotopic analysis and major ion chemistry could be important for studies of natural waters, but offer no practical suggestions as to a method of analysis. Here, I expand on the techniques of [2] and [19], to combine ion chemistry and isotope analyisis by using two tracers, one which acts conservatively, remaining in the liquid phase, and one that partitions between the liquid and vapor phases. I will compare the differences in the rates of return of the tracers to their background concentrations, and use their behaviors to estimate the fluxes of liquid- and vapor-phase water through the spring, heat energy partitioning, and several other variables that characterize the spring's mass and energy balance.

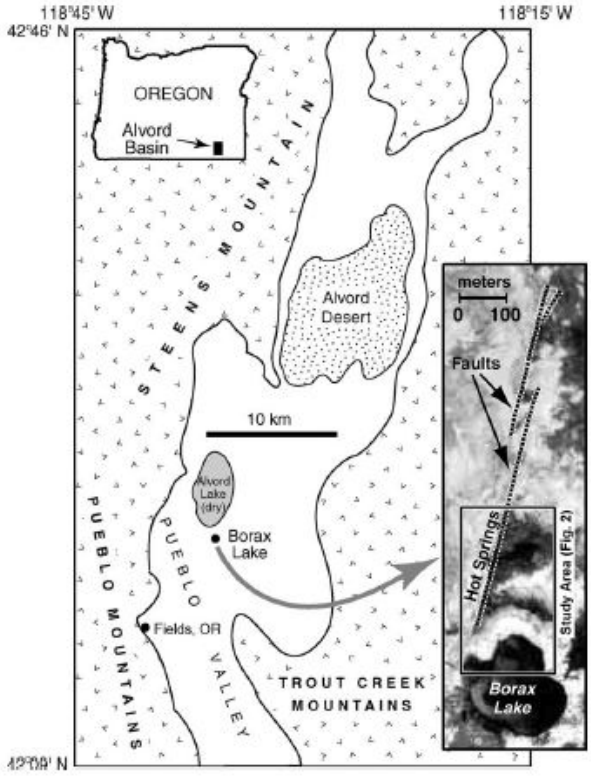

Figure 1.1: Map of the Alvord Basin with Borax Lake, spring locations north of the lake. Taken from [8]

1.2 Site Information

To execute the experiment for this study, I chose two hot springs, B1180 and B1210,[1] located in the Alvord Basin at the Borax Lake Thermal Area (BLTA), southeast Oregon, because of its desolate location away from people, ease of spring access, and prior knowledge of study area. The BLTA contains approximately 175 fault-controlled hot springs which are linearly-aligned along the trace of the Borax Lake Fault and range in temperature from 31-94 ℃ [8]. Previous studies indicate the springs originate from a common reservoir and experience no mixing with shallow, cool groundwaters [7].

[1]Spring identifiers as used by [8].

CHAPTER 2

Methods

2.1 Model Development

The model I develop here is a variation of the well-known 'salt tank mixing problem' described in most ordinary differential equations textbooks; for example, see [9]. In this type of mixing problem, water is entering a tank at a certain rate and concentration and water is leaving the tank at a certain rate and concentration (usually these values are different than the initial values). The key assumption in this system is that the concentration of salt in the water leaving the tank represents the well-mixed concentration at any given time and, when solved, the solution is represented by exponential decay such as the model used by [2].

Using mass balance, the governing equations for the two tracers are expressed as follows:

$$\frac{dC}{dt} = \frac{r_{in}}{v}C_{in} - \frac{r_{out}}{v}C(t), \tag{2.1}$$

$$\frac{d\delta}{dt} = \frac{r_{in}}{v}\delta_{in} - \frac{r_{out}}{v}\delta(t) - \frac{r_e}{v}\delta_e, \tag{2.2}$$

In equation (2.1), C is the concentration of the conservative tracer in the spring [M/M][1], here chloride, and t is time [T]. C_{in} is the concentration of chloride in the water entering the spring and $C(t)$ is the well-mixed concentration of chloride in the spring at any time, t. r_{in} and r_{out} are the rates of liquid water entering and leaving the spring respectively [L^3/T], and v is the volume of the spring [L]. Both equations are of similar form and r_{in}, r_{out}, t, and v are the same values, however, an additional term is necessary in equation (2.2) to represent the fraction of the non-conservative tracer, deuterium, that is leaving by evaporation in the vapor phase, r_e [L^3/T]. δ is value of the ratio of the heavy to light isotope ($D/^1H$), normalized to a standard, VSMOW, δ_{in} is the δ-value of water entering the spring, δ_e is the δ-value of the

[1]Dimensional units are M = mass, T = time, and L = length

vapor leaving by evaporation, and $\delta(t)$ is the δ-value of the well-mixed spring water at any time t (δ-values to be discussed in a future section). In this model, changes in density and volume are negligible over the temperature and concentrations of the experiment so they are neglected from the model.

To reduce these equations to their simplest, functional form dimensionless parameters are defined and a new governing equation is formed. From this, a class of models emerges that use the same form of the following general governing equation:

$$\frac{d\theta}{d\tau} = A_1 - A_2\theta(\tau), \tag{2.3}$$

with the initial condition:

$$\theta(\tau = 0) = A_3, \tag{2.4}$$

where θ is the non-dimensional representation of the tracer in the well-mixed spring water normalized to the initial, spiked value, τ is dimensionless time, and A_1, A_2, and A_3 are constants specific to a process being modelled and each constant will take on a different value once the process is specified. Here I am modelling the equations with and without the effects of evaporation on mass transfer as shown in equations (2.1) and (2.2).

Equations of this form can be easily solved by direct integration and the general solution takes on the form of

$$\theta = A_4 + A_5 e^{-A_6\tau}, \tag{2.5}$$

where A_4, A_5, and A_6 are constants that describe the different process(es) controlling the abundance of tracer in the spring water. Each model will be described seperately in the following sections.

2.1.1 Chloride mass balance model

By using the conservative ion chloride, the process of evaporation is largely neglected to obtain equation (2.1). To non-dimensionalize equation (2.1), the following dimensionless parameters are defined:

$$\theta_{Cl} = \frac{C(t)}{C(t=0)}, \tag{2.6}$$

$$\theta_{in,Cl} = \frac{C(in)}{C(t=0)}, \tag{2.7}$$

$$\epsilon = \frac{r_{in}}{r_o}, \tag{2.8}$$

$$\tau = \frac{t}{t_c}, \tag{2.9}$$

$$t_c = \frac{v}{r_o}, \tag{2.10}$$

Following the notation described in section 2.1, θ_{Cl} is the dimensionless representation of the chloride concentration in the spring water at any time ($C(t)$) normalized to the value the moment after spiking the concentration ($C(t=0)$), $\theta_{in,Cl}$ is the non-dimensional concentration of chloride in the water entering the spring (Cl_{in}) normalized to the spiked concentration ($C(t=0)$), ϵ is the ratio of water entering and leaving the spring (r_{in} and r_{out} respectively), and τ is the dimensionless time normalized to the spring's characteristic time (the amount of time until the chloride concentration has returned to $\frac{1}{e}$ above the measured background concentration). A springs characteristic time is controlled by the effective mixing volume and the rate of discharge

Sustituting the dimensionless parameters above for the dimensional parameters in equation (2.1) gives the following non-dimensional governing equation:

$$\frac{d\theta_{Cl}}{d\tau} = \epsilon\theta_{in,Cl} - \theta_{Cl}, \tag{2.11}$$

with the initial condition:

$$\theta_{Cl}(\tau = 0) = 1, \tag{2.12}$$

Equation (2.11) states that the change in chloride concentration over time is porportional to the chloride concentration of the incoming water and the ratio of how quickly water is entering and leaving the spring minus the well-mixed chloride concentration in the spring water. Because the dimensionless concentration is normalized to the spiked concentration, the intial condition specifies that the non-dimensional chloride concentration is equal to 1 at the start of the experiment ($t = 0$), which is the highest value it can obtain non-dimensionally.

As noted in section 2.1, equation (2.11) can be solved using direct integration and the non-dimensional general solution is:

$$\theta_{Cl} = \epsilon\theta_{in,Cl} - A_7 e^{-\tau}, \tag{2.13}$$

with the initial condition:

$$\theta_{Cl}(\tau = 0) = 1, \tag{2.14}$$

where A_7 is the constant of integration. Substituting the intial condition and solving for A_7, the unique solution for the chloride balance model is:

$$\theta_{Cl} = \epsilon\theta_{in,Cl} - (\epsilon\theta_{in,Cl} - 1)e^{-\tau}, \tag{2.15}$$

with the initial condition:

$$\theta_{Cl}(\tau = 0) = 1, \tag{2.16}$$

Once calibrated, equation (2.15) estimates the non-dimensional concentration of chloride at any time, τ. At the start of the experiment when $C(t) = C(t = 0)$, $\theta = 1$, as previously mentioned, but equation (2.15) reveals that over a long period of time, such that $\tau \to \infty$, $\theta = \epsilon\theta_{in,Cl}$ regardless of the concentration at the start of the experiment, in other words the chloride concentration will asymptotically return to the background value.

2.1.2 Chloride model parameterization

To calibrate the chloride model to each spring, parameters must be measured when able and estimated, calculated, or assumed when they cannot. For the springs sampled at the BLTA, measureable paramaters include the concentration of chloride in the spring before the spike ($C(t < 0)$ or background), concentration of the well-mixed spring water just after the spike ($C(t = 0)$), and time (t). The characteristic time (t_c) is found by plotting the measured chloride concentrations against time and matching the time when the concentration has returned to $\frac{1}{e}$, or 0.37, above the measured background chloride concentration, see Figures (2.1) and (2.2). The effective mixing volume (v) is the volume of water that makes up a spring and most of which resides in the subsurface [2] and [23], and [19], this value is different than the volume calculated in the field which only represents the volume of spring water visible from the surface. The effective mixing volume is calculated by the following relationship presented by [19]:

$$\Delta C = \frac{M}{v} \tag{2.17}$$

that is, the change in concentration (C mg/L) experienced by the spike is porportional to the amount added (M mol) and the volume (v L) it was added into. The values obtained for the characteristic time and volume are used in the relationship described in equation (2.10) to estimate the rate at which liquid water is leaving the spring (r_o). Identifying t_c calibrates τ to the spring and then the measured non-dimensional values can be compared to the values predicted by the exponential decay model, see Figure (3.1) and (3.2). Lastly, ϵ is calculated by the relationship defined in equation (2.8) to estimate the rate at which water is entering the spring (r_{in}) after the calibration of the deuterium model (described in section 2.1.4).

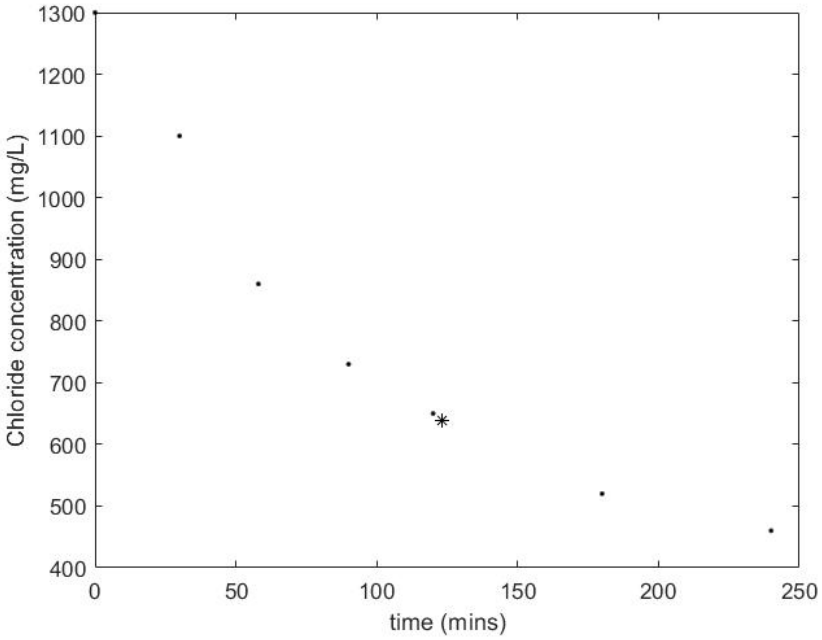

Figure 2.1: Chloride concentration for B1180 as a function of time (.) and (*) marks when C is $\frac{1}{e}$ above background.

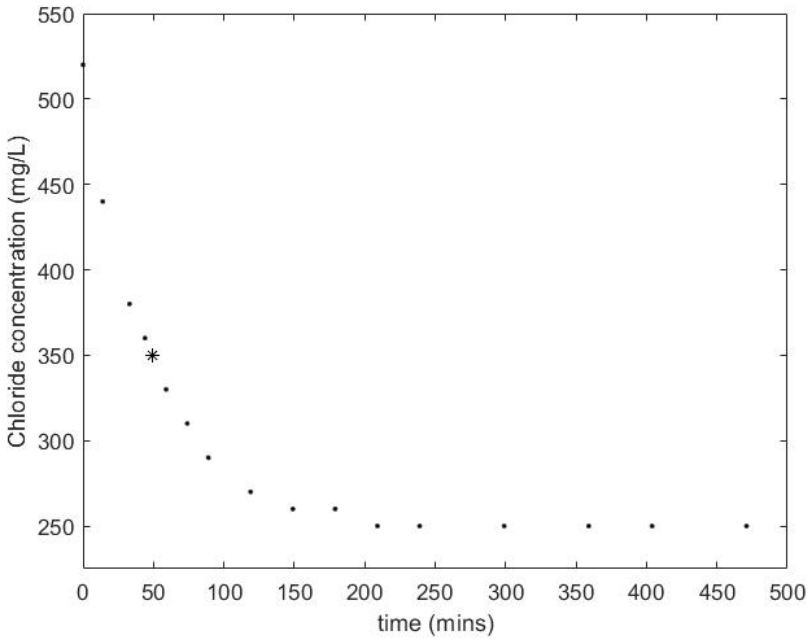

Figure 2.2: Chloride concentration for B1210 as a function of time (.) and (*) marks when C is $\frac{1}{e}$ above background.

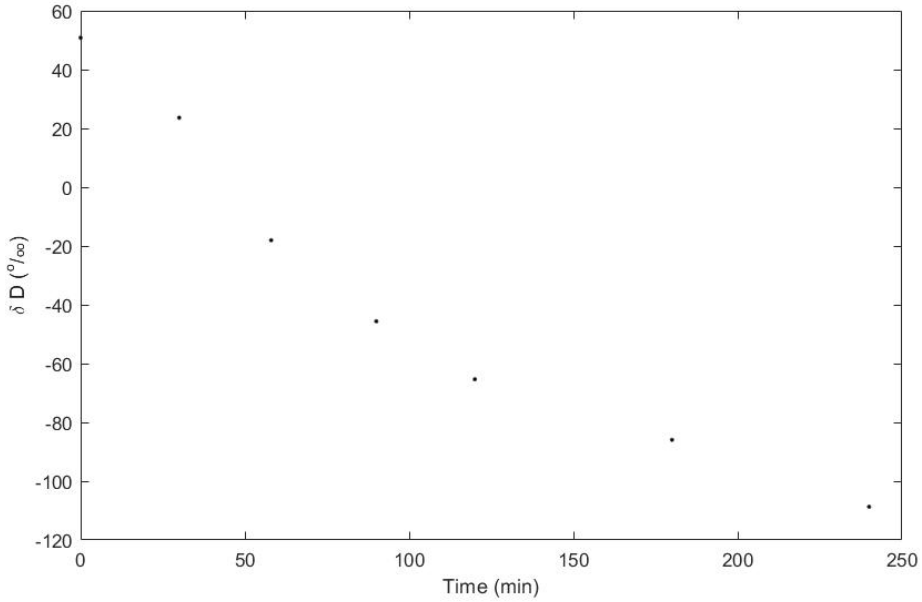

Figure 2.3: δD values for spring B1180 as a function of time.

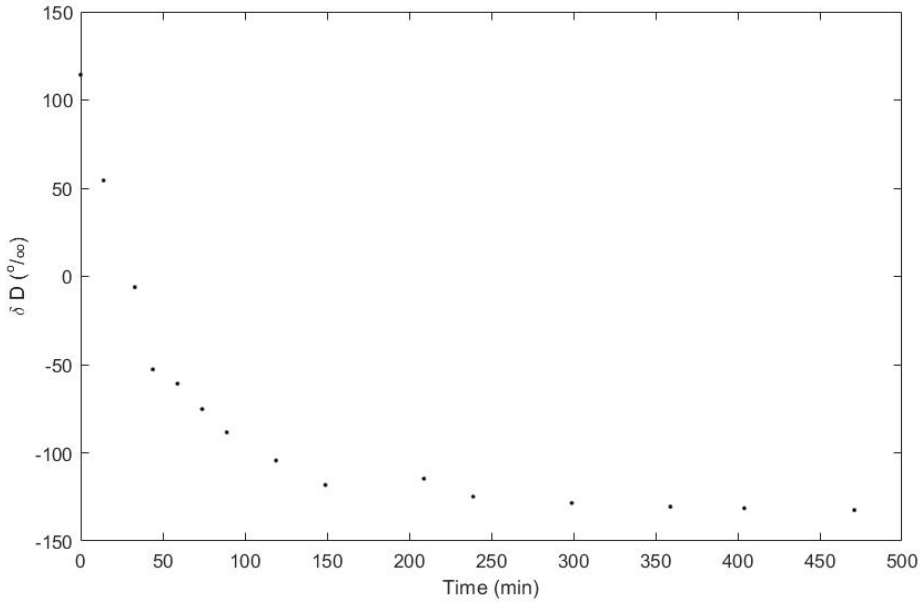

Figure 2.4: δD values for spring B1210 as a function of time.

2.1.3 Deuterium mass balance model

For the portion of the model that applies to the non-conservative tracer, which partitions with water vapor during evaporation, the stable isotope deuterium is chosen. The δ-value for a stable isotope is described by [3], [5], [24], and others as the following relationship:

$$\delta = \left[\frac{R_a}{R_s} - 1\right] \times 1000 \tag{2.18}$$

where R is the ratio of heavy to light isotopes ($D/^1H$), R_a and R_s are the ratios in the sample and the reference standard respectively. The standards used in this study are VSMOW, VSLAP, and WAWA.

To account for the loss of mass due to evaporation, I use the following substitution given by [12] to describe the isotopic composition of water removed by evaporation:

$$\delta_e = \frac{1}{(1-h+\Delta E)}\left[\frac{E}{\alpha} - h\delta_A - \Delta E\right] + \frac{\delta(t)}{\alpha(1-h+\Delta E)} \tag{2.19}$$

where h is the relative humidity, α is the equilibrium fractionation factor, E is the equilibrium enrichment factor, ΔE is the kinetic enrichment factor, and δ_A is the δ-value of the vapor in the atmosphere. After substituting equation (2.18) into equation (2.2), the dimensional governing equation is:

$$\frac{d\delta}{dt} = \frac{r_{in}}{V}\delta_{in} - \frac{r_e}{V}\left[\frac{1}{1-h+\Delta E}\left(\frac{E}{\alpha} + h\delta_A + \Delta E\right) - \frac{r_o}{V}\left(\frac{r_e}{r_o\alpha(1-h+\Delta E}\right) + 1\right]\delta_t \tag{2.20}$$

Defining the following non-dimensional parameters:

$$\theta_D = \frac{\delta(t)}{\delta(t=0)}, \tag{2.21}$$

$$\theta_{in,D} = \frac{\delta_{in}}{\delta(t=0)}, \tag{2.22}$$

$$\epsilon = \frac{r_{in}}{r_o}, \tag{2.23}$$

$$\beta = \frac{r_e}{r_o}, \tag{2.24}$$

$$\tau = \frac{t}{t_c} \tag{2.25}$$

From 2.1, θ_D is the dimensionless representation of the δ-value in the spring water at any time ($\delta(t)$) normalized to the value the moment after spiking the spring ($\delta(t=0)$), $\theta_{in,D}$ is the dimensionless representation of the δ-value of the water entering the spring (δ_{in}) normalized to the spiked value ($\delta(t=0)$), and β is the ratio of water leaving as vapor by evaporation and the water leaving as liquid (r_e and r_{out} respectively). ϵ, τ, and t_c are the same values defined in section 2.1.2.

Once again, using the methods described in section 2.1.1 and the defined non-dimensional parameters the dimensionaless form of the governing equation (2.19) is :

$$\frac{d\theta_D}{d\tau} = \epsilon\theta_{in,D} + \beta\left[\frac{1}{1-h+\Delta E}\left(\frac{E}{\alpha} + h\delta_A + \Delta E\right)\right] - \left[\left(\frac{\beta}{\alpha(1-h+\Delta E}\right)+1\right]\theta_D(\tau), \tag{2.26}$$

with initial condition:

$$\theta_D(\tau=0) = 1 \tag{2.27}$$

As before, equation (2.25) describes, non-dimensionally, how the δ-value of deuterium changes with time, however, it is clear that there is an extra term in the constant A_2 from equation (2.3). This term arises because deuterium fractionates during evaporation and leaves the spring with water vapor. Once again, the deuterium model is normalized to the

spiked δ-value so that at the start of the experiment the non-dimensional δ-value is at the highest value allowed, 1.

By using direct integration to solve equation (2.25), the following non-dimensional general solution is found:

$$\theta_D = \frac{A_8}{A_9} + A_{10} e^{-A_9 \tau} \tag{2.28}$$

with initial condition:

$$\theta_D(\tau = 0) = 1 \tag{2.29}$$

where:

$$A_8 = \epsilon\theta_{in,D} + \beta\left[\frac{1}{1-h+\Delta E}\left(\frac{E}{\alpha} + h\delta_A + \Delta E\right)\right] \tag{2.30}$$

$$A_9 = \left[\left(\frac{\beta}{\alpha(1-h+\Delta E}\right) + 1\right] \tag{2.31}$$

and A_{10} is the constant of integration. One last substitution is necessary before obtaining the unique solution.

$$\lambda = \left[\frac{1}{1-h+\Delta E}\left(\frac{E}{\alpha} + h\delta_A + \Delta E\right)\right] \tag{2.32}$$

$$\gamma = \left[\left(\frac{\beta}{\alpha(1-h+\Delta E}\right) + 1\right] \tag{2.33}$$

After applying the above substitutions and the initial condition, the final form of the non-dimensional solution for the deuterium model is:

$$\theta_D = \frac{\epsilon}{\gamma}\theta_{in,D} + \frac{\beta\lambda}{\gamma} + \left[1 - \left(\frac{\epsilon}{\gamma}\theta_{in,D} + \frac{\beta\lambda}{\gamma}\right)\right] e^{-\lambda\tau}; \tag{2.34}$$

with initial condition:

$$\theta_D(\tau = 0) = 1 \tag{2.35}$$

Once parameterized, equation (2.33) estimates the non-dimensional δ-value at any time, τ. At the start of the experiment when the δ-value of the well mixed spring water is equal to the spiked δ-value ($\delta(t) = \delta(t = 0)$), the non-dimensional δ-value (θ_D) is equal to one, as previously mentioned, but, as before, equation (2.33) reveals that over a long period of time, such that $\tau \to \infty$, the values will asymptotically return to background, $\theta = \frac{\epsilon}{\gamma}\theta_{in,D} + \frac{\beta\lambda}{\gamma}$, regardless of the δ-value at the start of the experiment.

2.1.4 Deuterium model parameterization

The paramaters for the deuterium model are found in the same manner as the chloride model: by measurement, estimation, or calculation. Albeit most are difficult to obtain because isotopic fractionation rates and δ-values greatly differ depending on geographic location and are typically found by calibration. Measureable paramaters are relative humidity (h), time (t), the background δ-value ($\delta(t = 0)$), and the δ-values at each sample time ($\delta(t)$). γ is a fitting parameter that is estimated when the dimensionless measured δ-values are fit to the model values calculated in section 2.1.3. t_c and r_{out} are the values of characteristic time and rate of liquid water leaving the springs, respecively, that are estimated from section 2.1.1.

Isotope fractionation in bodies of water is governed by two known processes: equilibrium fractionation and kinetic enrichment [12]. Equilibrium fractionation is a well-known process of how isotopes fractionate due to differences in mass between two isotopologues and the values for equilibrium fractionation factors (α) are readily available for an assortment of stable isotopes at almost any range of temperatures. In this study, the α-values are from [18] and calculated at the spring temperature. I chose values from [18] because they are the most used values in water isotope studies [12], [11], and [17]. Kinetic enrichment is

isotopic fractionation due to differences in transport resistance between the heavy and light isotopolgues in air and has been related to the molecular diffusivities at the water-atmosphere interface. The kinetic enrichment factor (ΔE) used in the deuterium model is calculated from [4] using :

$$\Delta E = (1 - h)(\frac{\rho_i}{\rho}) \tag{2.36}$$

where h is the humidity and ρ and ρ_i are the resistance coefficients of the light and heavy isotope respectively. The value for $(\frac{\rho_i}{\rho})$ is also given by [4] as 1.0083. The values calculated from equation (2.36) are 0.0091 and 0.0073 for B1180 and B1210 respectively.

2.2 Chemistry

To obtain the measurements needed in the models, two hot springs in the BLTA, B1180 and B1210, were chosen and sampled on September 22, 2018. Spring and air temperatures were collected using a handheld thermometer affixed with a K-type thermocouple. Using a tape measure, the spring diameter and depth were carefully measured as to not disturb the walls of the spring. Using the measured spring depth and diameter, the visible spring volume was calculated. The relative humidity of the air was measured using an Extech RH390 Precision Thermo Hygrometer.

Water samples were collected using a polyethylene tube with a single-hole rubber stopper affixed at one end and the sampling tube was marked for consistent sampling depths, half of the estimated spring depth. Chloride samples were filtered using a 0.45μm filter. Both chloride and deuterium samples were sealed, seperately, with paraffin inside centrifuge tubes and stored out of light until they were analyzed at the lab. No reagents were added to the samples. Tracers were added to the springs following methods by [2] and [19]. Before the start of the experiment, two background water samples were collected from each spring then, at a predetermined time, each spring was dosed simultaneously with known amounts

of KCL and pure D_2O, then stirred with a collapsible oar to encourage complete mixing. The springs were sampled in regular time intervals to obtain the well-mixed concentrations of each tracer as they returned to background concentrations (see [19] for detailed sampling procedures). Samples were analyzed for Cl^- at the University of Idaho Analytical Sciences Laboratory using a Dionex DX-100 Ion Chromatograph. The δD samples were analyzed at GeoAnalytical Laboratory at Washington State University using a Thermo Delta V Plus IR-MS and the following standards for reference: VSMOW, VSLAP, and WAWA following procedures by [19].

CHAPTER 3

Results

3.1 Results

As mentioned, on September 22, 2018, at the BLTA several parameters were monitored throughout the day such as relative humidty (%) and air temperature (°C), these values can be found in Table (3.1). The value used for relative humidity in the model is a weighted average of measured relative humidity during each experiment (9.5% for B1180 and 14.0% for B1210). Spring temperatures were measured at the start and end of each experiment and can be found in Table (3.2). Spring temperatures for B1180 were 70.8°C and 68.3°C at the beginning and end of the experiment respectively and 94.0°C and 93.3°C for B1210 at the start and end of the experiment respectively.

Time series and measured background values for both springs can be found in Table (3.3). As expected, the values of the tracers are high immediately after doping and both tracers decrease towards background for the remainder of the experiment. Time series sample data are presented graphically in Figures (2.1) through (2.4).

The time series sample data are compared to the values calculated from the models presented here and are found in Figures (3.1) and (3.2). Using the model fits, estimates for the following parameters are obtained: t_c, γ, and ϵ. These values along with the calibration parameters and estimated mixing volume (v) are tabulated in Table (3.4).

Rates of water entering and leaving the springs as liquid and vapor are estimated using the models. The rate of water entering the spring is 4.3766 and 7.49 L/min for B1180 and B1210 respectively, liquid water is discharging at a rate of 4.2593 and 7.2720 L/min for B1180 and B1210 respectively. Water leaving the springs by vapor is leaving the springs at a rate of 0.1173 and 0.2200 L/min for B1180 and B1210 respectively. Additionally, the models allow for the chloride and δ-value of the water entering the spring to be calculated. For B1180 these values are C_{in}=243 mg/L and δ_{in}= -127.15 ‰ and for B1210 these values

Table 3.1: Relative humidity and air temperature.

Time	RH (%)	Air Temp (°C)
09:15	21.7	20.2
09:50	20.9	23.5
10:25	17.8	23.8
10:30	17.5	23.8
11:00	16.6	26.6
13:20	9.2	31.4
16:48	9.1	27.6
17:19	9.1	25.8
18:40	10.5	24.2

Table 3.2: Spring temperatures measured at the beginning and end of each experiment.

	B1210	B1180
Time	Temp (°C)	Temp (°C)
10:30	94.0 (start)	
13:30		70.8 (start)
18:50	93.3 (end)	
19:00		68.3 (end)

Table 3.3: Elapsed time with corresponding chloride concentrations and δD. * indicates points removed from the model.

B1210 Time (min)	B1210 Cl^- (mg/L)	B1210 δD (‰VSMOW)	B1180 Time (min)	B1180 Cl Cl^- (mg/L)	B1180 δD (‰VSMOW)
Background	250	-134.401	Background	250	-161.272
0	520	114.3185	0*	3800	561.9064
14	440	54.38961	15*	3100	441.5912
33	380	-6.11747	30*	2400	295.5936
44	360	-52.7236	45*	2000	219.6368
59	330	-60.8562	60*	1700	160.8828
74	310	-75.2476	75	1300	50.8336
89	290	-88.4066	105	1100	23.6316
119	270	-104.389	133	860	-18.024
149	260	-118.26	165	730	-45.5972
179	260		195	650	-65.3404
209	250	-114.652	255	520	-85.942
239	250	-124.834	315	460	-108.705
299	250	-128.448			
359	250	-130.595			
404	250	-131.454			
471	250	-132.481			

Table 3.4: Parameter values used in the models. [(1)] from [18] [(2)] from [12]

Parameter:	$\alpha^{(1)}$	$\Delta E^{(2)}$	h	t_c (min)	γ	ϵ	v (L)
B1180	1.03655	0.0091	0.095	123	0.975	1.0275	524
B1210	1.03655	0.0073	0.12	49	0.95	1.0303	356

Table 3.5: Parameters calculated from the calibrated model.

Parameter:	r_{in} (L/min)	r_{out} (L/min)	r_e (L/min)	C_{in} (mg/L)	δ_{in} (‰)
B1180	4.3766	4.2593	0.1173	243	-127.15
B1210	7.49	7.2720	0.2200	242	-123.93

are C_{in}=242 mg/L and δ_{in}= -123.93 ‰. Characteristics of the incoming water can be found in Table (3.5).

Figure 3.1: Spring B1180: Measured non-dimensional chloride concentration (blue dots) and δ D (black dots) as a function of dimensionless time (τ) compared to the model values (solid black for chloride and solid purple for deuterium.

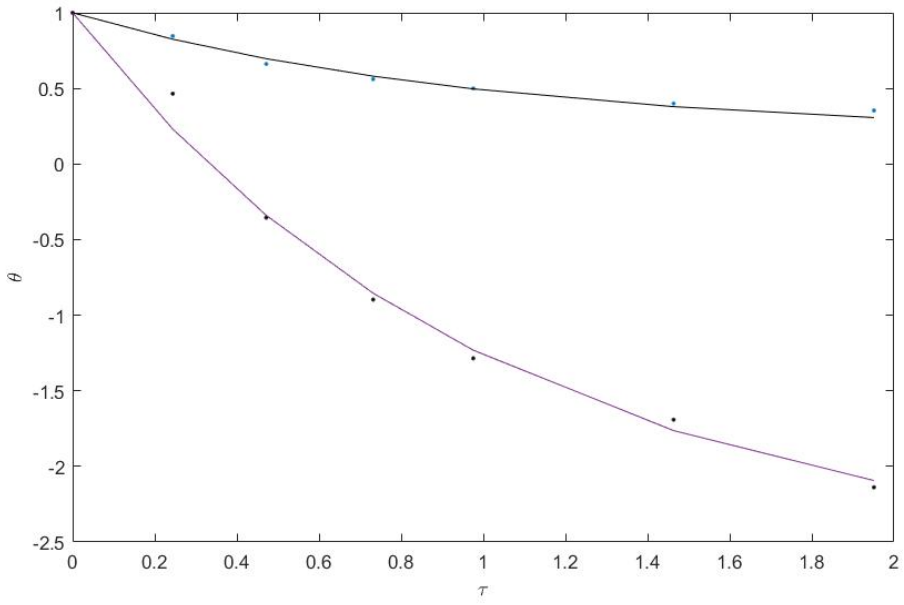

Figure 3.2: Spring B1210: Measured non-dimensional chloride concentration (blue dots) and δ D (black dots) as a function of dimensionless time (τ) compared to the model values (solid black for chloride and solid purple for deuterium.

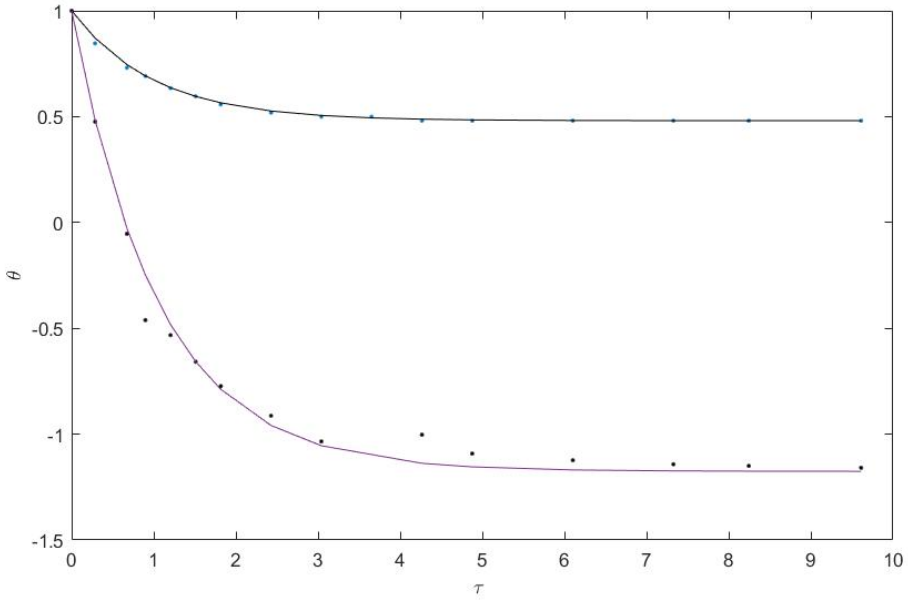

CHAPTER 4

Discussion

4.1 Discussion

Tracer methods have been used to estimate fluxes in springs for some time. [2] used this method in a hot spring in New Zealand and his results suggest that subsurface discharge accounts for up to three-quarters of the total discharge seen at the surface and the through-flow needed to support the surface heat balance model was almost identically matched using the (conservative) chloride tracer method. Later [19] improved on these methods by applying the doping method to springs in Yellowstone except this time the authors used the (non-conservative) stable isotope deuterium because of the sensitive ecosystem present in the park. The author showed that the prior method of estimating the heat flow for the Yellowstone caldera using the chloride inventory method by [20] and [13] neglects the heat transfered in the subsurface by advection since the chloride inventory method only measures surface discharge. Though the studies by [2] and [19] support and refine calculations for heat balances, there are errors built into their methods. In the study by [2], a conservative tracer was used to infer subsurface advection so there is no component in the model to account for heat transferred by evaporation. [19] uses a non-conservative tracer, however, their method also focuses on advective heat transfer even though the authors are aware that deuterium was undoubtedly lost to water vapor during evaporation. The result of neglecting the transfer of heat by evaporation builds error into the heat balance estimates. The goal of the present study is to use both conservative and non-conservative tracers to spike a hot spring then contrast the results to target the error introduced by the loss of mass through vapor.

The rates for water entering and leaving the springs indicate that the percent of mass leaving as liquid is 97.3% and 97.1% for B1180 and B1210, respectively, and the percent of mass leaving by evaporation is 2.7% and 2.9%, respectively. As expected, the amount of mass leaving the springs by evaporation is low and likely not significant for calcuating the

mass flux in hot springs. The amount of mass leaving by evaporation in spring B1210 is slightly higher than B1180 and is likely caused by the higher spring temperature observed for B1210/ (93.3℃ for B1210 and 70℃ for 1180) and the larger surface area measured, 9,974 cm^2 and 8,8281 cm^2 for B1210 and B1180 respectively.

On the basis of the mass flux calculations, the amount of heat transferred by spring water (advection) can be calculated using only one model as shown by authors mentioned here, but by contrasting two tracers an estimate for evaporation can be made and calculations for the amount of heat being carried away from the spring surface by evaporation (convection) can be made. Using the mass fluxes calculated in this study, the amount of heat transferred by advection for spring B1180 is approximetly $1.8x10^4$ J/s and by convection is $4.6x10^3$ J/s. The results are similar for B1210 with an advective heat flux of $4.2x10^4$ J/s and a convective flux by evaporation of $7.8x10^3$ J/s. These results imply that the percent of heat leaving by vapor is 16-20% when compared to advection for B1180 and B1210, respectively. Although the surface area for B1180 is 1,693 cm^2 smaller than B1210, the model suggests that during the experiment B1180 lost more heat to evaporation. This difference is likely because B1210 is protected by a dirt mound and vegetation whereas B1180 is more exposed to the atmosphere with much less vegetative cover (see Figure (8)). During the experiment the wind velocity increased significantly throughout the day and both springs experienced a drop in temperature, although the overall change was more for B1180 (ΔT = 2.5 ℃) when compared to B1210 (ΔT = 0.7 ℃). The convective heat transfer coefficient, h_a, is poportional to wind speed by way of the Reynolds Number [14] and the extent of the effect of wind speed on convective heat transfer at the hot spring surface should be investigated further. This method allows for the calcluation of mass like similar methods, however, it allows for a more thorough calulation of the energy losses by evaporation and suggests that by neglecting the transfer of heat during evaporation the total heat budgets are likely missing a fairly large component of the overall heat flux.

The method here allows us to determine other spring characteristics such as the effective

Figure 4.1: Spring B1180

Figure 4.2: Spring B1210

mixing volume, which is required for the model to be calibrated properly and I calculate an effective mixing volume of 524L and 356L for B1180 and B1210 respectively. As expected, and previously shown by authors mentioned, this contrasts with the estimated field volume calculated by measuring the springs surface area and estimated depth (46.1L and 38.3L B1180 and B1210 respectively). These values suggest that the springs have complex underground plumbing that is involved in mixing and is not observable at the surface. The tracer results for B1180 indicate that at the start of the experiment the spring water was not fully mixed such that first few values are unrealistically high (see Table 3.3). This is presumably because too much tracer was added and not enough time passed to allow for complete mixing. This is a phenomenom that [19] also experienced in their study and by removing data points until the data started fitting the model, the exponential curve is projected back to $t = 0$ to approximate the well-mixed values. We followed this method and after the first 5 values for B1180 are removed, the data fits the model curve and estimates the discharge for B1180 to be 4.3 L/min and the characteristic time is 123 minutes. These estimates are lower than B1210, 7.27 L/min and 49 minutes for discharge and characteristic time respectively, in spite

of B1180 having a larger observable and calucated effective mixing volume.

The models presented here predicts chloride concentration and the δD value of the water entering the spring in the subsurface. The values for chloride are 243.30 and 242.66 mg/L for B1180 and B1210 respectively. The predicted chloride concentrations are in good agreement with each other and the measured background concentrations (250 mg/L). The lower value of chloride in the incoming water when compared to the background concentration is expected because the rates of water leaving the spring is less than the rate of water coming into the spring and the conservative nature of chloride means it stays in the dissolved phase and will concentrate in the spring water; this is by definition the behavoir described by a salt tank problem. The predicted δD are also in agreeance between the springs, -127.15 and -123.93 ‰ for B1180 and B1210 respectively, and again these values differ from the well-mixed spring water, however for different reasons than the chroride concentrations. Deuterium is known to fractionate during evaporation and the isotopically light species (^1H) is preferrentially removed from the liquid water leaving the water in the spring enriched in the heavier isotope (D) and thus a more negative δD value. These values also agree with the δD value published by [8] for the geothermal well located a short distance away from the springs, about -126 ‰.

The models described here can be extended to other tracers as well such as iodine, as used by [23], oxygen (O^{18}) isotopes or others.. Once the calibrating parameters are known, such as the effective mixing volume and the characteristic time, the only parameter necessary to use the model is the background value for the tracer of interest in the well-mixed spring water. From the estimate of the effective mixing volume and the molecular weight of the tracer, a hypothetical spiked concentration can be calculated. Using the springs characteristic time, the model is calibrated to predict the rate at which background levels are achieved. This is important because the values can be adjusted to obtain estimates of incoming concentrations or δ-values for other tracers of interest.

4.2 Uncertainties

Although I think the major heat transfer processes are accounted for in my caluclations of heat flux, there are some processes that are neglected. For example, [21] showed that the land surface is important to geothermal production and can be quantified by use of the Biot number, a representation of the rate that heat is being supplied to the surface and how quickly it is being taken away by convection. In this study, direct convective cooling to the air is likely small but possibly not-negligible and is likely important for calculating the energy budget in hot springs. The effect of conductive heat lost to the soils directly from the hot spring wall is also likely to add a small amount to the overall heat budget as demonstrated by [16]. Radiative heating and cooling by the sun is also neglected from the heat flux calculations. The effect of these processes are lumped into the overall error of the model and are likely small.

CHAPTER 5

Conclusion

5.1 Conclusion

The study presented here uses two tracers, a conserative tracer, chloride, and a non-conservative tracer, deuterium, to investigate the heat and mass transfer between the vapor and liquid phases in two hot springs in the Borax Lake Therma Area in southeast Oregon. The model estimates parameters such as the effective mixing volume, the rate of liquid water entering the springs in the subsurface, the concentrations of chloride and δD values in the incoming waters, and can be extended to other tracers of interest. The results presented in this model can be useful in calculating characteristics of the deeper reservoir and suggestions for future areas of work are given. Furthermore, our investigation suggests that the effect of evaporation on mass transport is negligible but it has a great effect on energy transport in hot springs. The model suggests that the springs experience approximetely 97.1-97.3 % loss of mass in the liquid leaving the springs and only about 2.7-2.9 % loss in mass by evaporation but showed that evaporation accounts for at least 16-20% of the total heat transferred from the spring. This study will be useful for developing a more accurate thermal budget than has previously been possible.

References

[1] T. Anderson and J. Fairley, Journal of Geophysical Research **113** (2008) page B05402

[2] R. Benseman, Journal of Geophysical Research **64** (1959) page 1063-1065

[3] H. Craig , Science **133** (1961) page 1702-1703

[4] H. Craig and L. Gordon, Consiglio nazionale delle richerche, Laboratorio de geologia nucleare Pisa (1965)

[5] R. Criss, Oxford University Press on Demand (1999)

[6] A. Ellis and S. Wilson, New Zealand Journal of Science and Technology **8** (1955) page 622-631

[7] J. Fairley, J. Heffner, and J. Hinds, Geophysical Research Letters **30** (2003)

[8] J. Fairley and K. Nicholson, Journal of Hydrology **231** (2006) page 276-285

[9] J. Fairley, John Wiley & Sons (2016)

[10] P. Finkelstein and P. Sims, Journal of Geophysical Research: Atmospheres **106.D4** (2001) page 3503-3509

[11] W. Giggenbach, Geochemica et Cosmochimica Acta **42** (1978) page 979-988

[12] R. Gonfiantini, Handbook of environmental isotope geochemistry, the terrestrial environment **2** (1986) page 113-168

[13] S. Hurwitz, R. Harris, C. Werner, and F. Murphy, Journal of Geophysical Research: Solid Earth **117** (2012)

[14] T. Bergman, F. Incropera, D. Dewitt, and A. Lavine, John Wiley & Sons (2011)

[15] I. Kocabas, Geothermics **34** (2005) page 27-46

[16] B. Lubenow, J. Fairley, C. Lindsey, and P. Larson, Journal of Volcanology and Geothermal Research **323** (2016) page 53-61

[17] B. Luz, E. Barkan, R. Yam, and A. Shemesh, Geochemica et Cosmochimica Acta **73** (2009) page 6697-6703

[18] M. Majoube, Journal de Chimie Physique et de Physico-Chimie Biologique **68** (1971) page 1423-1436

[19] N. McMillan, P. Larson, J. Fairley, J. Mulvaney-Norris, and C. Lindsey, Geosphere **14** (2018) page 1860-1874

[20] D. Norton and I. Friedman, Journal of Volcanology and Geothermal Research **26** (1985) page 231-250

[21] A. Price, C. Lindsey, and J. Fairley, Water Resources Research **53** (2017) page 10173-10187

[22] K. Pruess and C. Doughty, Lawrence Berkley National Lab (2010)

[23] J. Rowe, R. Fournier, and G. Morey, Geological Survey Research **Chapter B** (1965) page B184-B186

[24] Z. Sharp (2017)